

# Multiradar Data Fusion for Respiratory Measurement of Multiple People

Shunsuke Iwata, *Student Member, IEEE*, Takato Koda, and Takuya Sakamoto, *Senior Member, IEEE*,

**Abstract**—This study proposes a data fusion method for multiradar systems to enable measurement of the respiration of multiple people located at arbitrary positions. Using the proposed method, the individual respiration rates of multiple people can be measured, even when echoes from some of these people cannot be received by one of the radar systems because of shadowing. In addition, the proposed method does not require information about the positions and orientations of the radar systems used because the method can estimate the layout of these radar systems by identifying multiple human targets that can be measured from different angles using multiple radar systems. When a single target person can be measured using multiple radar systems simultaneously, the proposed method selects an accurate signal from among the multiple signals based on the spectral characteristics. To verify the effectiveness of the proposed method, we performed experiments based on two scenarios with different layouts that involved seven participants and two radar systems. Through these experiments, the proposed method was demonstrated to be capable of measuring the respiration of all seven people by overcoming the shadowing issue. In the two scenarios, the average errors of the proposed method in estimating the respiration rates were 0.33 and 1.24 respirations per minute (rpm), respectively, thus demonstrating accurate and simultaneous respiratory measurements of multiple people using the multiradar system.

**Index Terms**—Biomedical engineering, data fusion, radar measurement, radar imaging, radar signal processing.

## I. INTRODUCTION

**R**ESPIRATORY measurements have become increasingly important in a variety of applications, including healthcare, home medication, medical alert systems for babies, and monitoring systems used for infants and senior citizens. A variety of sensors and systems have been developed for these applications to monitor patient respiration [1]–[3] and among these systems, radar-based systems have been attracting attention as a promising approach because they are suitable for performing long-term measurements without patient discomfort since there is no need for the patient to wear a device. A number of existing studies have been reported on the measurement of people using radar techniques, including systems for estimation of the locations of people [4]–[9], tracking of

people in motion [10]–[17], and detection of patient vital signs, including their heartbeat and respiration [18]–[38].

Another advantage of radar-based respiratory measurement is the possibility of performing simultaneous measurements of the respiration of multiple people using only a single device. There have been numerous studies in which a single radar system has been used to measure the respiration of multiple people [18]–[36]. For example, Nosrati et al. [33], Islam et al. [34], Su et al. [35], and Koda et al. [36] used single radar systems to demonstrate simultaneous measurement of the respiration of two, three, three, and seven people, respectively. These studies, however, did not consider the effect of the shadowing problem, in which an echo from one target person is blocked by another person located between the first person and the radar system; this results in the radar system being unable to detect a person (or some people) when multiple people are present in the scene.

To overcome the shadowing problem, this study introduces simultaneous use of multiple radar systems to perform respiratory measurements of multiple people. There have been previous studies that used multiple radar systems to measure the respiration of multiple people: Shang et al. [37] used two radar systems to measure two people in the presence of body motion, and Yang et al. [38] also used two radar systems to measure five people. In these studies, it was assumed that the relative positions and orientations of the radar systems were known in advance, and that the echoes from all target people could be measured directly by each of the radar systems without the shadowing problem. These assumptions, however, cannot always be satisfied in practice, which hinders the use of the radar-based respiratory measurement approach in actual daily environments.

As discussed above, none of the existing studies have accounted for the effect of the shadowing problem, which prevents the echo from one person from being detected by one of the radar systems. In this study, we propose a novel multiradar data fusion method to perform respiratory measurements that can measure multiple people simultaneously. The proposed method can mitigate the effect of the shadowing problem using multiple radar systems without knowing the relative locations and orientations of these radar systems. The proposed method generates multiple radar images using the multiradar data, and these radar images are then converted into multiple sets of two-dimensional point clouds. To align these point clouds, the proposed method then estimates the relative positions and orientations of the multiple radar systems, which allows for

This study was supported in part by JSPS KAKENHI under Grants 19H02155 and 21H03427, JST PRESTO under Grants JPMJPR1873, and JST COI under Grants JPMJCE1307.

S. Iwata, T. Koda and T. Sakamoto are with the Department of Electrical Engineering, Graduate School of Engineering, Kyoto University, Kyoto, Kyoto, 615-8510 Japan.

data fusion of the multiradar system and thus overcomes the shadowing problem. The proposed method even works when the positional relationships among the multiple radar systems are unknown, which means that there is no requirement for calibration to be performed beforehand, and also no restriction on the physical installation of the radar systems. The performance of the proposed method is evaluated quantitatively by performing radar measurements involving seven participants and a pair of radar systems.

## II. IMAGING AND CLUSTERING OF HUMAN TARGETS USING MULTIPLE RADAR SYSTEMS

We assume use of a multiradar system comprising  $M$  radar systems with positions and angles that are unknown. Each radar system contains a  $K$ -element array (or virtual array). Let  $s_i(t, r)$  denote the signal received by the  $i$ -th element ( $i = 0, 1, \dots, K-1$ ) of the array, where  $t$  is the slow time and the range  $r$  is expressed as  $r = ct'/2$  using the fast time  $t'$  and the speed of light  $c$ . A signal vector  $\mathbf{s}(t, r)$  is defined as  $\mathbf{s}(t, r) = [s_0(t, r), s_1(t, r), \dots, s_{K-1}(t, r)]^T$ , where the superscripted T represents a transpose operator. We assume here that all elements of the array antennas are calibrated and that static clutter is suppressed by subtracting the time-averaged signal.

Using the  $m$ -th radar system ( $m = 1, \dots, M$ ), a radar image is generated and is expressed in the two-dimensional Cartesian coordinate system  $(x_m, y_m)$ , where the  $x_m$  axis is aligned with the array baseline of the  $m$ -th radar system. A complex radar image  $I_m(t, \mathbf{r}_m)$  is generated from the  $m$ -th radar system's data as  $I_m(t, \mathbf{r}_m) = \mathbf{w}(\phi_m)^H \mathbf{s}(t, \rho_m)$ , where  $\mathbf{r}_m$  is the position vector that can be expressed as  $(x_m, y_m)$  in Cartesian coordinates and as  $(\rho_m, \phi_m)$  in polar coordinates. The weight vector is  $\mathbf{w}(\theta) = [w_0, w_1, \dots, w_{K-1}]^T$ , where the choice of  $w_i$  depends on the imaging algorithm being used. In this study, we use a straightforward beamformer (BF) method for simplicity, in which the weights are set as  $w_i(\theta) = \alpha_i e^{-j(2\pi x_i/\lambda) \sin \theta}$  ( $i = 0, 1, \dots, K-1$ ). Here, we use the Taylor window coefficient  $\alpha_i$ . Fig. 1 shows a system model containing multiple radar systems for measurement of multiple human targets, in which we see that each radar system has its own coordinate system.

Next, a point cloud is generated from each radar image; the  $m$ -th point cloud is generated randomly to follow a density distribution that is proportional to  $\rho_m |I_m(t, \mathbf{r}_m)|^2$ , where  $\rho_m$  is introduced to compensate for propagation losses. The X-means clustering technique [36], [39] is then applied to the point cloud and the clusters  $c_1, c_2, \dots, c_N$  are generated; these clusters correspond to the  $N$  targets. For presentation purposes, we generated a radar cluster image  $C_m(t, \mathbf{r}_m)$  that takes the values  $\{0, 1, 2, \dots, N\}$ , which correspond to the indices of the clusters  $c_1, c_2, \dots, c_N$  except for 0;  $C_m(t, \mathbf{r}_m) = 0$  indicates that no cluster is associated with  $\mathbf{r}_m$ . Finally, the representative position  $\mathbf{r}_m^{(i)}$  of cluster  $c_i$  in the  $m$ -th radar image is calculated [36]; the clusters' representative

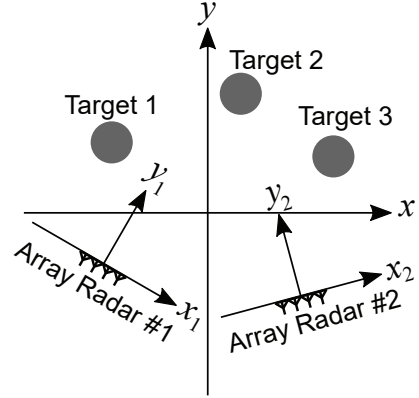


Fig. 1. Schematic of system model for measurement of multiple target people using multiple radar systems.

positions are then processed in the proposed data fusion algorithm, which combines multiple radar images.

## III. MULTIRADAR DATA FUSION FOR RESPIRATORY MEASUREMENT OF MULTIPLE PEOPLE

The main issue when performing radar measurements of multiple human targets indoors is that not all of these human targets can be measured directly using only a single radar system because of shadowing, i.e., where one human echo is blocked by another human target or by obstacles; this occurs frequently when multiple people are located together and are densely spaced. To mitigate this issue, we use a multiradar system to increase the probability that at least one of these radar systems can detect all human targets in the scene. Given the radar images  $I_m(t, \mathbf{r}_m)$  and the cluster positions  $\mathbf{r}_m^{(i)}$  for  $m = 1, \dots, M$ , we propose a data fusion method here that combines the multiple radar images. Here, we assume a special case with  $M = 2$  for simplicity. The first step in the method is to find a rigid transformation that can align the coordinates from the  $x_2$ - $y_2$  coordinate system to those of the  $x_1$ - $y_1$  coordinate system.

### A. Procrustes Analysis for Alignment of Associated Target Clusters

We propose a data fusion method that uses Procrustes analysis [40] to find the rigid transformation parameters required to describe the relationship between two sets of points in a plane. Let us assume here that  $N$  pairs of two-dimensional vectors  $(\mathbf{r}_1^{(1)}, \mathbf{r}_2^{(1)}), (\mathbf{r}_1^{(2)}, \mathbf{r}_2^{(2)}), \dots, (\mathbf{r}_1^{(N)}, \mathbf{r}_2^{(N)})$  correspond to  $N$  pairs of points. The purpose of this section is to find a rigid transformation that adjusts the points  $\mathbf{r}_2^{(n)}$  ( $n = 1, \dots, N$ ) with respect to  $\mathbf{r}_1^{(n)}$  ( $n = 1, \dots, N$ ). If appropriate transformation parameters are selected, the points are then transformed to satisfy  $\mathbf{r}_1^{(n)} \simeq R\mathbf{r}_2^{(n)} + \mathbf{t}$  using the translation vector  $\mathbf{t}$  and the rotation matrix  $R$ . If we subtract the average coordinates  $\bar{\mathbf{r}}_m = (1/N) \sum_{n=1}^N \mathbf{r}_m^{(n)}$  ( $m = 1, 2$ ) from the position vectors using  $\tilde{\mathbf{r}}_m^{(n)} = \mathbf{r}_m^{(n)} - \bar{\mathbf{r}}_m$ , we can then simplify the problem for large  $N$ ; we need only

estimate the  $R$  that satisfies  $\tilde{\mathbf{r}}_1^{(n)} = R\tilde{\mathbf{r}}_2^{(n)}$ . Here, we define  $2 \times N$  matrices  $S_1$  and  $S_2$  as:

$$S_1 = [\tilde{\mathbf{r}}_1^{(1)}, \tilde{\mathbf{r}}_1^{(2)}, \dots, \tilde{\mathbf{r}}_1^{(N)}], \quad (1)$$

$$S_2 = [\tilde{\mathbf{r}}_2^{(1)}, \tilde{\mathbf{r}}_2^{(2)}, \dots, \tilde{\mathbf{r}}_2^{(N)}], \quad (2)$$

and we estimate a rotation matrix  $R^*$  as:

$$R^* = \underset{\text{subject to } R^T R = I, \det R = 1,}{\arg \min_R} \|S_1 - RS_2\|_F^2, \quad (3)$$

where the subscripted F denotes the Frobenius norm and represents the square root of the sum of squares of all components.

In the Procrustes analysis, rather than solve for the optimization problem in Eq. (3) directly, singular value decomposition is used to estimate  $R^*$ ;  $S_1 S_2^T$  is decomposed using the form  $S_1 S_2^T = U \Sigma V^T$ , where  $U$  and  $V$  are  $2 \times 2$  orthogonal matrices, and  $\Sigma$  represents a  $2 \times 2$  diagonal matrix with non-negative real numbers. We then obtain the rotation matrix  $R^* = UV^T$ . Using  $R^*$ , the position vector  $\tilde{\mathbf{r}}_2^{(n)}$  is transformed to give  $R^* \tilde{\mathbf{r}}_2^{(n)} + \bar{\mathbf{r}}_1$ , which is a mapping from the coordinate system  $x_2$ - $y_2$  to the coordinate system  $x_1$ - $y_1$ . Although we have discussed the special case where  $M = 2$  above, a similar procedure can be performed in a general case, including cases where  $M > 2$ .

### B. Proposed Data Fusion Method Using Respiratory Correlation and Procrustes Analysis

To apply Procrustes analysis to transformation of the coordinate systems of a multiradar system, the cluster positions can be used to form the input matrices  $S_1$  and  $S_2$ . We should note here that Procrustes analysis requires at least two pairs of corresponding points, e.g.,  $(\mathbf{r}_1^{(1)}, \mathbf{r}_2^{(1)}), (\mathbf{r}_1^{(2)}, \mathbf{r}_2^{(2)})$ . In this section, we propose a method to associate the cluster positions that uses the respiratory features of the human targets. In the proposed method, the similarity of the respiratory displacement waveforms is used to associate multiple echoes. Although we explain the procedure for the case where  $M = 2$  for simplicity, the procedure can be extended to a general case with  $M > 2$ . The proposed method comprises the following five steps.

- 1) Two pairs of corresponding points are estimated using the correlation coefficient for the respiratory displacement waveforms. For the position vectors  $\mathbf{r}_1^{(n_1)}$  and  $\mathbf{r}_2^{(n_2)}$ , the correlation coefficient is calculated as:

$$\rho_c(n_1, n_2) = (1/\rho_0) \int \angle I_1(t, \mathbf{r}_1^{(n_1)}) \angle I_2(t, \mathbf{r}_2^{(n_2)}) dt, \quad (4)$$

where  $\rho_0$  is introduced for normalization. First, we find a pair  $(n_1^*, n_2^*)$  that maximizes  $\rho_c(n_1, n_2)$ , where

$$(n_1^*, n_2^*) = \arg \max_{(n_1, n_2)} \rho_c(n_1, n_2). \quad (5)$$

Then, we find another pair  $(n_1^{**}, n_2^{**})$ , where

$$(n_1^{**}, n_2^{**}) = \underset{\text{subject to } n_1 \neq n_1^*, n_2 \neq n_2^*}{\arg \max_{(n_1, n_2)} \rho_c(n_1, n_2)}. \quad (6)$$

- 2) Procrustes analysis is applied to the two pairs of points  $(n_1^*, n_2^*)$  and  $(n_1^{**}, n_2^{**})$ , and the rigid transformation parameters  $R^*$  and  $\mathbf{t}^*$  are then obtained.
- 3) Using  $R^*$  and  $\mathbf{t}^*$ , all position vectors  $\mathbf{r}_m^n$   $m = 1, \dots, M; n = 1, \dots, N$  are transformed into the coordinate system  $x_1$ - $y_1$ . All pairs of transformed points separated by a distance of less than a threshold distance (i.e.,  $|\mathbf{r}_1^{(n_1)} - R^* \mathbf{r}_2^{(n_2)} - \mathbf{t}^*| \leq d_{th}$ ) are regarded as associated pairs.
- 4) All associated pairs are processed using the Procrustes analysis, and the transformation parameters  $R^*$  and  $\mathbf{t}^*$  are then updated.
- 5) For each human target, one of the displacements  $\angle I_1(t, \mathbf{r}_1^{(n_1)}), \dots, \angle I_M(t, \mathbf{r}_1^{(n_M)})$  is selected that is most likely to reflect the target's respiratory motion. We proposed selection of the displacement with the waveform that is closest to a sinusoidal wave. Using the following fourth-order moment of the power spectrum, we then find the  $m$  that maximizes  $\kappa(n, m)$  for each  $n$  ( $1 \leq n \leq N$ ). We define

$$\kappa(n, m) = \frac{\int_0^\infty \left| \int_{-\infty}^\infty I_m(t, \mathbf{r}_m^{(n)}) e^{-j\omega t} dt \right|^4 d\omega}{\left| \int_0^\infty \left| \int_{-\infty}^\infty I_m(t, \mathbf{r}_m^{(n)}) e^{-j\omega t} dt \right|^2 d\omega \right|^2}, \quad (7)$$

and the optimum  $m$  is then found as

$$m^*(n) = \arg \max_m \kappa(n, m), \quad (8)$$

which means that the  $m^*(n)$ -th radar signal is used for the  $n$ -th human target. As a result, the displacement waveform that is most likely to be related to their respiration is selected for each person, thus leading to accurate measurement of their respiration.

## IV. EXPERIMENTAL EVALUATION OF THE PROPOSED METHOD

### A. Multiradar Experiment with Multiple People

We performed the experiments using both a pair of array radar systems and belt-type respirometers simultaneously to evaluate the accuracy of the multiradar-based respiratory measurements acquired using the proposed method. To evaluate the accuracy of the method in measuring the respiratory intervals, all participants wore a belt-type respirometer on their upper torso. Each participant was seated and was breathing normally, and the measurements were acquired using two radar systems that were installed with different orientations and at different positions. Note that the belt-type respirometers were only used to evaluate the accuracy of the radar-based measurements.

Both radar systems are frequency-modulated continuous wave (FMCW) radar systems with a center frequency of 79 GHz, a center wavelength of  $\lambda = 3.8$  mm, and an occupied bandwidth of 3.9 GHz. The beamwidths of the individual radar array elements are  $\pm 4^\circ$  and  $\pm 35^\circ$  in the E- and H-planes, respectively. The radar array is composed of a multiple-input multiple-output (MIMO) array that contains three transmitting and four receiving elements,

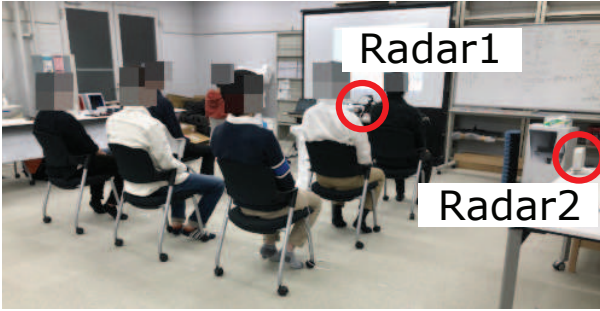


Fig. 2. Measurement setup with the seven seated participants shown with belt-type respirometer devices on their upper torsos in scenario 1.

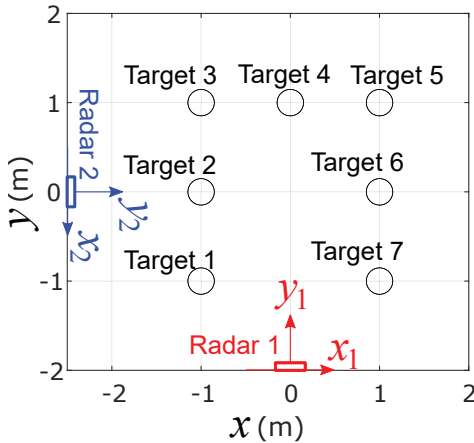


Fig. 3. Actual layout of the radar systems and the participants in scenario 1.

with spacings of 7.6 mm ( $2\lambda$ ) between the transmitting elements and spacings of 1.9 mm ( $\lambda/2$ ) between the receiving elements. In the experimental setting, the MIMO array can be approximated using a virtual linear array. Specifically, the array used in this study can be approximated using a 12-element virtual linear array with element spacings of  $\lambda/2$ . The slow-time sampling intervals were 100 ms.

We apply the proposed method to the radar data that were measured with the seven participants in two scenarios. We set different layouts for both the human targets and the radar systems in these scenarios. In scenario 1, as shown in Fig. 2, the seven participants were seated in a U-shaped arrangement with participant spacing of 1 m. We then used a pair of array radar systems to measure the participants as illustrated in Fig. 3. In scenario 2, the seven participants were seated in a different layout, as shown in Fig. 4, and the radar systems were also placed at different positions with different orientations, as illustrated in Fig. 5. The measurement time was set at 120 s and the participants were instructed to remain still and breathe normally during the measurements. To evaluate the accuracy of the respiration measurements, belt-type contact respirometers were used simultaneously with the radar measurements.

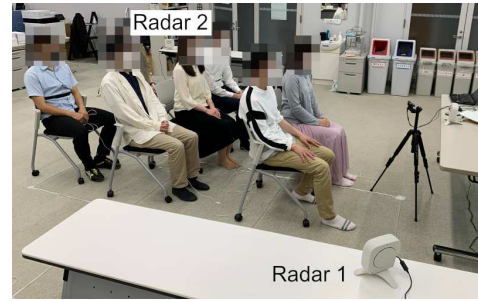


Fig. 4. Measurement setup with the seven seated participants shown with belt-type respirometer devices on their upper torsos in scenario 2.

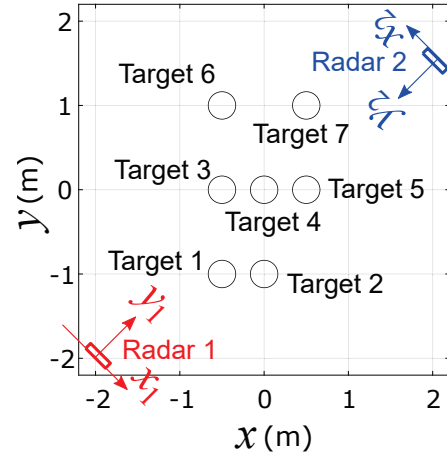


Fig. 5. Actual layout of the radar systems and the participants in scenario 2.

### B. Application of the Proposed Data Fusion Method to the Measured Radar Data

1) *Application in Scenario 1*: First, we apply the proposed method to the data acquired in scenario 1. The left and right panels of Fig. 6 show radar images  $|I_1(t, \mathbf{r}_1)|^2$  and  $|I_2(t, \mathbf{r}_2)|^2$  at  $t = 30$  s. In the figure, the actual target positions are indicated by white circles with the target numbers. Next, a point cloud is generated from these images and the respiratory-space clustering algorithm [36] is then applied to generate the radar cluster images  $|C_1(t, \mathbf{r}_1)|^2$  and  $|C_2(t, \mathbf{r}_2)|^2$  shown in Fig. 7. In the figure, an alphabetical label is provided for each cluster. In image  $|I_1(t, \mathbf{r}_1)|^2$  in Fig. 6, the echo from target 3 is barely visible because of shadowing; as a result, in Fig. 7, target 3 is not classified as a cluster. The resulting number of clusters was thus estimated erroneously to be six rather than seven, which is equivalent to the estimated number of human targets. This type of shadowing problem can occur particularly when multiple people are densely spaced within the measurement scene. To mitigate the shadowing problem, this study uses multiple radar systems rather than a single system.

Next, the proposed method is used to calculate the correlation coefficient  $\rho_C$  for each pair of displacement waveforms (see Table I). The proposed method finds two

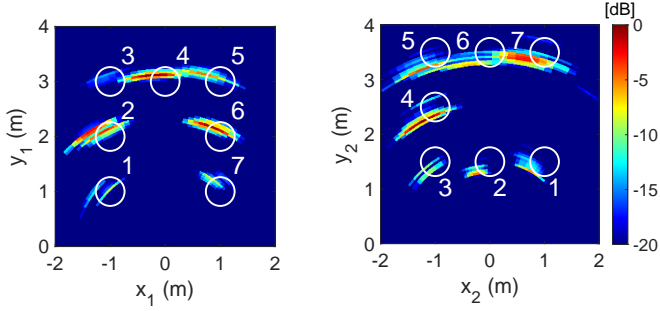


Fig. 6. Examples of radar images  $|I_1(t, \mathbf{r}_1)|^2$  (left panel) and  $|I_2(t, \mathbf{r}_2)|^2$  (right panel) at  $t = 30$  s in scenario 1.

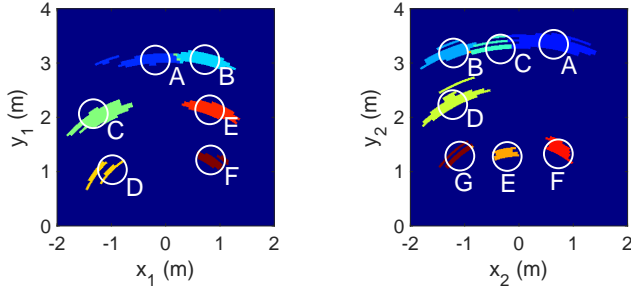


Fig. 7. Radar cluster images  $|C_1(t, \mathbf{r}_1)|^2$  (left panel) and  $|C_2(t, \mathbf{r}_2)|^2$  (right panel) at  $t = 30$  s in scenario 1. The different colors represent different clusters.

pairs of points with the largest and second largest values of  $\rho_C$ . In Table I, we can find the largest correlation coefficient for the pairing of target E (radar 1) and target C (radar 2). We can also find the second largest correlation coefficient for the pairing of target C (radar 1) and target E (radar 2). These pairs (E, C), (C, E) are processed via the Procrustes analysis for  $N = 2$  and the rigid transformation parameters  $x = -2.52$  m,  $y = 1.90$  m, and  $\theta = -1.58$  rad are obtained.

Using these parameters, the radar image  $|I_2(t, \mathbf{r}_2)|^2$  is then transformed into  $|\hat{I}_2(t, \mathbf{r}_1)|^2$ . Using the transformation parameters, the proposed method associates the six cluster pairs (A, D), (B, B), (C, E), (D, F), (E, C), and (F, A) from the seven human targets, where the distance threshold was set at  $d_{th} = 0.5$  m. Note that cluster G from the second radar system was not associated in this process. The associated pairs are then processed via the Procrustes analysis and the transformation parameters  $x = -2.46$  m,  $y = 1.86$  m, and  $\theta = -1.57$  rad are updated, as illustrated in Fig. 8.

For the associated cluster pair  $(n_1, n_2)$ , the respiratory displacement waveforms  $\angle I_1(t, \mathbf{r}_1^{(n_1)})$  and  $\angle I_2(t, \mathbf{r}_2^{(n_2)})$  are then obtained. The detection rate for 120 s for each target is shown in Table II. The table shows that human target 3 was not detected by one of the radar systems because of shadowing. All the human targets, with the exception of target 3, were detected by both radar systems, which gives us selection options; we can thus select a more accurate radar system for each target. In the proposed method, the fourth-order statistical parameter  $\kappa$  is calculated for

TABLE I  
CORRELATION COEFFICIENTS  $\rho$  FOR THE DISPLACEMENT WAVEFORMS IN SCENARIO 1

		Target index of radar 2						
		A	B	C	D	E	F	G
Target index of radar 1	A	0.13	0.63	0.02	0.15	0.01	0.17	0.07
	B	0.19	0.60	0.10	0.52	0.34	0.02	0.02
	C	0.20	0.05	0.04	0.03	0.81	0.01	0.01
	D	0.24	0.08	0.36	0.06	0.14	0.36	0.23
	E	0.18	0.07	0.89	0.04	0.15	0.13	0.80
	F	0.04	0.27	0.56	0.29	0.04	0.20	0.51
	G							

TABLE II  
TARGET DETECTION RATES IN SCENARIO 1

		Participant number						
		1	2	3	4	5	6	7
Radar 1 (%)		100	100	0	100	100	100	100
Radar 2 (%)		100	100	100	100	100	69	100
Proposed (%)		100	100	100	100	100	100	100

both displacement waveforms, from which the waveform with the larger  $\kappa$  value is selected every 30 s. Table V shows the errors in estimation of the respirations per minute (rpm) obtained when the two radar systems are combined. The error averaged over the seven participants is 0.33 rpm for the proposed process when combining the two radar systems. These results indicate that the proposed method using the multiradar system is effective in performing accurate respiration measurements of multiple people simultaneously.

2) *Application in Scenario 2:* We also applied the proposed method to the radar data acquired in scenario 2. The layout of the target people in this case is shown in Fig. 5. Using radar systems 1 and 2, the radar images  $|I_1(t, \mathbf{r}_1)|^2$

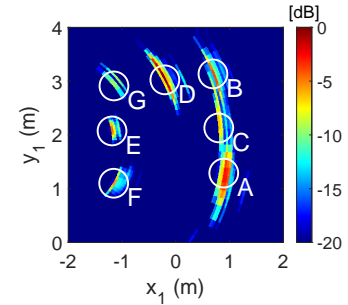


Fig. 8. Radar image  $|\hat{I}_2(t, \mathbf{r}_1)|^2$  after the optimized rigid transformation is performed in scenario 1.

TABLE III  
CORRELATION COEFFICIENTS  $\rho$  FOR THE DISPLACEMENT WAVEFORMS IN SCENARIO 2

		Target index of radar 2					
		A	B	C	D	E	F
Target index of radar 1	A	0.27	0.38	0.14	0.22	0.03	0.38
	B	0.01	0.14	0.36	0.03	0.02	0.20
	C	0.25	0.42	0.18	0.38	0.11	0.44
	D	0.31	0.04	0.29	0.21	0.35	0.15
	E	0.09	0.07	0.08	0.29	0.07	0.17
	F						

TABLE IV  
TARGET DETECTION RATES IN SCENARIO 2

	Participant number						
	1	2	3	4	5	6	7
Radar 1 (%)	100	100	100	100	0	58	72
Radar 2 (%)	0	100	100	100	100	100	100
Proposed (%)	100	100	100	100	100	100	100

and  $|I_2(t, \mathbf{r}_1)|^2$  were generated as shown in Fig. 9. We can then generate the radar cluster images  $|C_1(t, \mathbf{r}_1)|^2$  and  $|C_2(t, \mathbf{r}_2)|^2$  shown in Fig. 10. In Fig. 10, no clusters are generated for targets 5 and 6 because the echoes from targets 5 and 6 are weak in image  $|I_1(t, \mathbf{r}_1)|^2$ , as shown in Fig. 9. Similarly, no cluster is generated for target 1 because the echo is weak in image  $|I_2(t, \mathbf{r}_1)|^2$ , as shown in Fig. 9.

The proposed method is then used to calculate the correlation coefficient  $\rho_C$  for each of the pairs of displacement waveforms (Table III). In Table III, we find that the largest correlation coefficient is that for the pairing of target C (radar 1) and target F (radar 2), and also find that the second largest correlation coefficient is that for the pairing of target A (radar 1) and target B (radar 2). These pairs, denoted by (C,F), (A,B), are processed via the Procrustes analysis for  $N = 2$  and the rigid transformation parameters  $x = -0.17$  m,  $y = 5.11$  m, and  $\theta = -3.07$  rad are obtained.

Then, using these parameters, the radar image  $|I_2(t, \mathbf{r}_2)|^2$  is transformed into  $|\hat{I}_2(t, \mathbf{r}_1)|^2$ . Using the transformation parameters, the proposed method associates the four cluster pairs (A,B), (B,C), (C,F), and (E,D) from the clusters, where the distance threshold was set at  $d_{th} = 0.5$  m. Note that cluster D from the first radar system and clusters A and E from the second radar system were not associated in this process. Using the associated pairs, the transformation parameters  $x = 0.12$  m,  $y = 5.09$  m, and  $\theta = 3.06$  rad are updated, as illustrated in Fig. 11.

For the associated cluster pair  $(n_1, n_2)$ , the respiratory displacement waveforms  $\angle I_1(t, \mathbf{r}_1^{(n_1)})$  and  $\angle I_2(t, \mathbf{r}_2^{(n_2)})$  are obtained. The respiration detection rates for each target when using the proposed method are shown in Table IV, which shows that human targets 1 and 5 were only detected by one of the two radar systems because of shadowing, whereas the other targets were detected by both radar systems. As in scenario 1, the fourth-order statistical parameter  $\kappa$  is calculated for each of the estimated displacement waveforms, from which the waveform with the larger value of  $\kappa$  is selected every 30 s. Table V shows the errors in respiration rate estimation when using the proposed data fusion technique for these radar systems. The average error for the seven participants was 1.24 rpm when using the proposed method to combine the radar data.

## V. CONCLUSION

In this study, we have proposed a novel method for a multiradar system that can measure the positions and res-

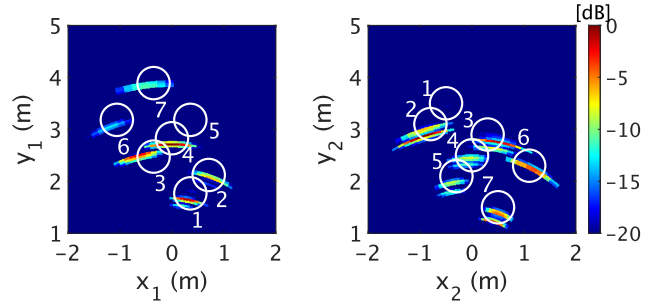


Fig. 9. Examples of radar images  $|I_1(t, \mathbf{r}_1)|^2$  (left panel) and  $|I_2(t, \mathbf{r}_2)|^2$  (right panel) at  $t = 30$  s in scenario 2.

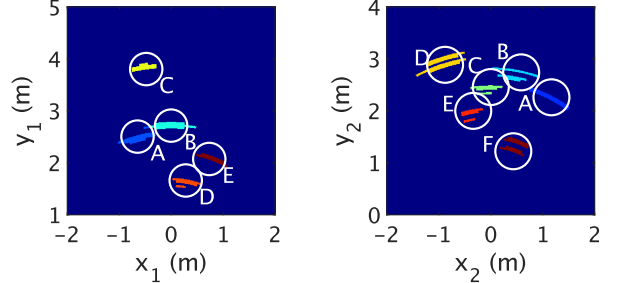


Fig. 10. Radar cluster images  $|C_1(t, \mathbf{r}_1)|^2$  (left panel) and  $|C_2(t, \mathbf{r}_2)|^2$  (right panel) at  $t = 30$  s in scenario 2. The different colors represent different clusters.

piration characteristics of multiple people. By introducing multiple radar systems rather than a single system, the shadowing problem can be mitigated, which means that the respiration rates of multiple people can be measured even when these people are located closely together. In addition, when using multiple radar systems, we can measure each person from multiple directions, which improves the accuracy of the respiration measurements. The effective-

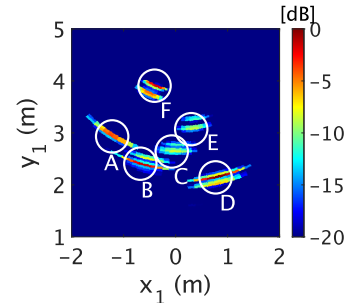


Fig. 11. Radar image  $|\hat{I}_2(t, \mathbf{r}_1)|^2$  after the optimized rigid transformation is performed in scenario 2.

TABLE V  
ERRORS IN RPM ESTIMATION WHEN USING THE PROPOSED METHOD

	Participant number						
	1	2	3	4	5	6	7
Scenario 1 (rpm)	0.43	0.02	0.06	0.88	0.72	0.05	0.15
Scenario 2 (rpm)	0.40	1.79	1.75	1.97	0.04	0.38	2.35

ness of the proposed method was verified experimentally in two scenarios using a pair of radar systems and seven participants.

In both scenarios, the proposed method was demonstrated to be able to detect all participants by combining the data acquired from the two radar systems, whereas not all participants could be detected when using only one of the two radar systems because of shadowing. The average respiratory rate estimation error for the seven participants in the two scenarios was 0.79 rpm, which is sufficiently small when compared with the typical respiration rate range for adults (12-20 rpm). Use of the multiradar system with the proposed method has been demonstrated to be promising for use in accurate noncontact monitoring of the respiration of multiple people.

#### ACKNOWLEDGMENT

We thank Dr. Hirofumi Taki and Dr. Shigeaki Okumura of MaRI Co., Ltd. for their help with this study.

#### REFERENCES

- [1] M. Ali, A. Elsayed, A. Mendez, Y. Savaria, M. Sawan, and M. Sawan, "Contact and remote breathing rate monitoring techniques: A review," *IEEE Sensors J.*, early access, Apr. 12, 2021, DOI: 10.1109/JSEN.2021.3072607.
- [2] C. Massaroni, A. Nicolò, M. Sacchetti, and E. Schena, "Contact-less methods for measuring respiratory rate: A review," *IEEE Sensors J.*, vol. 21, no. 11, pp. 12821–12839, Jun. 2021.
- [3] A. Singh, S. U. Rehman, S. Yongchareon, and P. H. J. Chong, "Multi-resident non-contact vital sign monitoring using radar: A review," *IEEE Sensors J.*, vol. 21, no. 4, pp. 4061–4084, Nov. 2020.
- [4] L. Storrer, H. C. Yildirim, E. P. Copa, J. Louveaux, P. De Doncker, S. Pollin, and F. Horlin, "Experimental implementation of a multi-antenna 802.11ax-based passive bistatic radar for human target detection," in *Proc. IEEE Radar Conf.*, Florence, Italy, Sept. 2020, pp. 1–6.
- [5] A. Abuduaini, N. Shiraki, N. Honma, T. Nakayama, and S. Iizuka, "Performance evaluation of multiple human-body localization using bistatic MIMO radar," in *Proc. IEEE Asia-Pacific Microw. Conf. (APMC)*, Singapore, Dec. 2019, pp. 575–577.
- [6] T. Ha and J. Kim, "Detection and localization of multiple human targets based on respiration measured by IR-UWB radars," in *Proc. IEEE SENSORS*, Montreal, Canada, Oct. 2019, pp. 1–4.
- [7] N. Honma, D. Sasakawa, N. Shiraki, T. Nakayama, and S. Iizuka, "Human monitoring using MIMO radar," in *Proc. IEEE Int. Workshop Electromagn.:Appl. Stud. Innov. Compet. iWEM*, Nagoya, Japan, Aug. 2018, pp. 1–2.
- [8] G. Shingu, K. Takizawa, and T. Ikegami, "Human body detection using MIMO-UWB radar sensor network in an indoor environment," in *Proc. 9th Int. PDCAT*, Dunedin, New Zealand, Dec. 2008, pp. 437–442.
- [9] J. W. Choi, D. H. Yim, and S. H. Cho, "People counting based on an IR-UWB radar sensor," *IEEE Sensors J.*, vol. 17, no. 17, pp. 5717–5727, Sept. 2017.
- [10] S. S. Ram, Y. Li, A. Lin, and H. Ling, "Human tracking using Doppler processing and spatial beamforming," in *Proc. IEEE Radar Conf.*, Waltham, MA, USA, Apr. 2007, pp. 546–551.
- [11] D. Sasakawa, N. Honma, K. Nishimori, T. Nakayama, and I. Shoichi, "Evaluation of fast human localization and tracking using MIMO radar in multi-path environment," in *Proc. IEEE 27th Ann. Int. Symp. Pers., Indoor, Mobile Radio Commun. (PIMRC)*, Valencia, Spain, Sept. 2016, pp. 1–6.
- [12] S. Chang, R. Sharan, M. Wolf, N. Mitsumoto, and J. W. Burdick, "UWB radar-based human target tracking," in *Proc. IEEE Radar Conf.*, Pasadena, CA, USA, May 2009, pp. 1–6.
- [13] Y. He, F. Le Chevalier, and A. G. Yarovoy, "Association of range-Doppler video sequences in multistatic UWB radar for human tracking," in *Proc. 9th Eur. Radar Conf.*, Amsterdam, Netherlands, Nov. 2012, pp. 218–221.
- [14] A. E. Mitchell, G. E. Smith, K. L. Bell, and M. Rangaswamy, "Single target tracking with distributed cognitive radar," in *Proc. IEEE Radar Conf.*, Seattle, WA, USA, May 2017, pp. 0285–0288.
- [15] J. Rovnáková and D. Kocur, "Data fusion from UWB radar network: Preliminary experimental results," in *Proc. 21st Int. Conf. Radioelektronika*, Brno, Czech Republic, Apr. 2011, pp. 1–4.
- [16] G. L. Charvat, J. Goodwin, M. Tobias, J. Pozderac, and J. Peabody, "Detection algorithm implementation and measured results for a real-time, through-wall radar system using a TDM MIMO antenna array," in *Proc. IEEE Radar Conf.*, Atlanta, GA, USA, May 2012, pp. 0240–0246.
- [17] M. Shin and H. Son, "Multiple sensor linear multi-target integrated probabilistic data association for ultra-wide band radar," *IEEE Access*, vol. 8, pp. 227161–227171, 2020.
- [18] Y. Wang, Q. Liu, and A. E. Fathy, "Simultaneous localization and respiration detection of multiple people using low cost UWB biometric pulse Doppler radar sensor," in *Proc. IEEE MTT-S Int. Microw. Symp. Dig.*, Montreal, QC, Canada, Jun. 2012, pp. 1–3.
- [19] Q. Wu, Z. Mei, Z. Lai, D. Li, and D. Zhao, "A non-contact vital signs detection in a multi-channel 77GHz LFM CW radar system," *IEEE Access*, vol. 9, pp. 49614–49628, 2021.
- [20] D. –M. Chian, C. –K. Wen, F. –K. Wang, and K. –K. Wong, "Signal separation and tracking algorithm for multi-person vital signs by using Doppler radar," *IEEE Trans. Biomed. Circuits Syst.*, vol. 14, no. 6, pp. 1346–1361, Dec. 2020.
- [21] O. Boric-Lubecke, V. M. Lubecke, A. Host-Madsen, D. Samardzija, and K. Cheung, "Doppler radar sensing of multiple subjects in single and multiple antenna systems," in *Proc. 7th Int. Conf. Telecommun Modern Satellite, Cable and Broadcasting Services*, Nis, Serbia, Sept. 2005, vol. 1, pp. 7–11.
- [22] Y. Chen, H. Tan, B. Hu, and Y. Li, "Doppler radar based non-contact multi-person respiration signals separation," in *Proc. IEEE-EMBS Int. Conf. Biomed. Health Informatics*, Hong Kong, China, Jan. 2012, pp. 799–802.
- [23] S. M. M. Islam, E. Yavari, A. Rahman, V. M. Lubecke, and O. Boric-Lubecke, "Separation of respiratory signatures for multiple subjects using independent component analysis with the JADE algorithm," in *Proc. 40th Ann. Int. Conf. IEEE Eng. Med. Biol. Soc. (EMBC)*, Honolulu, HI, USA, Jul. 2018, pp. 1234–1237.
- [24] N. V. Rivera, S. Venkatesh, C. Anderson, and R. M. Buehrer, "Multi-target estimation of heart and respiration rates using ultra wideband sensors," in *Proc. 14th Eur. Signal Process. Conf.*, Florence, Italy, Sept. 2006, pp. 1–6.
- [25] M. Muragaki, S. Okumura, K. Maehara, T. Sakamoto, M. Yoshioka, K. Inoue, T. Fukuda, H. Sakai, and T. Sato, "Noncontact respiration monitoring of multiple closely positioned patients using ultra-wideband array radar with adaptive beamforming technique," in *Proc. IEEE ICASSP*, New Orleans, LA, USA, Mar. 2017, pp. 1118–1122.
- [26] C. Lu, Y. Yuan, C. –H. Tseng, and C. –T. Michael Wu, "Multi-target continuous-wave vital sign radar using 24 GHz metamaterial leaky wave antennas," in *Proc. IEEE MTT-S Int. Microw. Biom. Conf. (IMBioC)*, Nanjing, China, May 2019, pp. 1–4.
- [27] C. Ding, J. Yan, L. Zhang, H. Zhao, H. Hong, and X. Zhu, "Noncontact multiple targets vital sign detection based on VMD algorithm," in *Proc. IEEE Radar Conf.*, Seattle, WA, USA, May 2017, pp. 0727–0730.
- [28] H. Lv, M. Liu, T. Jiao, Y. Zhang, X. Yu, S. Li, X. Jing, and J. Wang, "Multi-target human sensing via UWB bio-radar based on multiple antennas," in *Proc. IEEE Reg. 10 Ann. Int. Conf. Proc. (TENCON)*, Xi'an, China, Oct. 2013, pp. 1–4.
- [29] A. Rittiplang and P. Phasukkit, "UWB radar for multiple human detection through the wall based on Doppler frequency and variance statistic," in *Proc. 12th Int. Conf. Biomed. Eng. (BMEiCON)*, Ubon Ratchathani, Thailand, Nov. 2019, pp. 1–5.
- [30] J. Yan, H. Hong, H. Zhao, Y. Li, C. Gu, and X. Zhu, "Through-wall multiple targets vital signs tracking based on VMD algorithm," *Sensors*, vol. 16, no. 8, p. 1293, 2016.

- [31] I. Walterscheid, O. Biallawons, and P. Berens, "Contactless respiration and heartbeat monitoring of multiple people using a 2-D imaging radar," in *Proc. 41st Ann. Int. Conf. IEEE Eng. Med. Biol. (EMBC)*, Berlin, Germany, Jul. 2019, pp. 3720–3725.
- [32] J. Xiong, H. Hong, H. Zhang, N. Wang, H. Chu, and X. Zhu, "Multitarget respiration detection with adaptive digital beamforming technique based on SIMO radar," *IEEE Trans. Microw. Theory Techn.*, vol. 68, no. 11, pp. 4814–4824, Nov. 2020.
- [33] M. Nosrati, S. Shahsavari, S. Lee, H. Wang, and N. Tavassolian, "A concurrent dual-beam phased-array Doppler radar using MIMO beamforming techniques for short-range vital-signs monitoring," *IEEE Trans. Antennas Propag.*, vol. 67, no. 4, pp. 2390–2404, Apr. 2019.
- [34] S. M. M. Islam, O. Boric-Lubecke, and V. M. Lubecke, "Concurrent respiration monitoring of multiple subjects by phase-comparison monopulse radar using independent component analysis (ICA) with JADE algorithm and direction of arrival (DOA)," *IEEE Access*, vol. 8, pp. 73558–73569, 2020.
- [35] W. Su, M. Tang, R. E. Arif, T. Horng, and F. Wang, "Stepped-frequency continuous-wave radar with self-injection-locking technology for monitoring multiple human vital signs," *IEEE Trans. Microw. Theory Techn.*, vol. 67, no. 12, pp. 5396–5405, Dec. 2019.
- [36] T. Koda, T. Sakamoto, S. Okumura, and H. Taki, "Noncontact respiratory measurement for multiple people at arbitrary locations using array radar and respiratory-space clustering," *IEEE Access*, July 2021 (accepted for publication).
- [37] X. Shang, J. Liu, and J. Li, "Multiple object localization and vital sign monitoring using IR-UWB MIMO radar," *IEEE Trans. Aerosp. Electron. Syst.*, vol. 56, no. 6, pp. 4437–4450, Dec. 2020.
- [38] Y. Yang, J. Cao, X. Liu, and X. Liu, "Multi-breath: Separate respiration monitoring for multiple persons with UWB radar," in *Proc. IEEE 43rd Ann. Comput. Softw. Appl. Conf. (COMPSAC)*, Milwaukee, WI, USA, Jul. 2019, pp. 840–849.
- [39] D. Pelleg and A. Moore, "X-means : Extending K-means with efficient estimation of the number of clusters," in *Proc. 17th Int. Conf. on Machine Learning*, Stanford, CA, USA, Jun. 2000, pp. 727–734.
- [40] J. M. F. Ten Berge, "J.C. Gower and G.B. Dijkstra-huis.Procrustes problems. New York: Oxford University Press," *Psychometrika*, vol. 70, no. 4, pp. 799–801, Dec. 2005.

#### ETHICS DECLARATIONS

This study was approved by the Ethics Committee of the Graduate School of Engineering, Kyoto University (permit no. 201916). Informed consent was obtained from all participants in the study.



**Shunsuke Iwata** (STM'21) received a B.E. degree in electrical and electronic engineering from Kyoto University, Kyoto, Japan, in 2021. He is currently working toward the M.E. degree in electrical engineering at the Graduate School of Engineering, Kyoto University. Mr. Iwata is a recipient of 2020 IEEE AP-S Kansai Joint Chapter Best Presentation Award. His research interests include multiradar measurement of respiration of multiple people.



**Takato Koda** received a B.E. degree in electrical and electronic engineering from Kyoto University, Kyoto, Japan, in 2020. He is currently working toward the M.E. degree in electrical engineering at the Graduate School of Engineering, Kyoto University. His research interests include radar imaging and clustering of multiple people using array radar systems.



**Takuya Sakamoto** (M'04–SM'17) received a B.E. degree in electrical and electronic engineering from Kyoto University, Kyoto, Japan, in 2000, and M.I. and Ph.D. degrees in communications and computer engineering from the Graduate School of Informatics, Kyoto University, in 2002 and 2005, respectively.

From 2006 to 2015, he was an Assistant Professor at the Graduate School of Informatics, Kyoto University. From 2011 to 2013, he was also a Visiting Researcher at Delft University of Technology, Delft, the Netherlands. From 2015 to 2018, he was an Associate Professor at the Graduate School of Engineering, University of Hyogo, Himeji, Japan. In 2017, he was also a Visiting Scholar at the University of Hawaii at Manoa, Honolulu, HI, USA. Since 2018, he has been a PRESTO Researcher at the Japan Science and Technology Agency, Kawaguchi, Japan. At present, he is an Associate Professor at the Graduate School of Engineering, Kyoto University. His current research interests are system theory, inverse problems, radar signal processing, radar imaging, and wireless sensing of vital signs.

Dr. Sakamoto was a recipient of the Best Paper Award from the International Symposium on Antennas and Propagation (ISAP) in 2012, and the Masao Horiba Award in 2016. In 2017, he was invited as a semi-plenary speaker to the European Conference on Antennas and Propagation (EuCAP) in Paris, France.